



Melatonin Attenuates Dasatinib-Aggravated Hypoxic Pulmonary Hypertension via Inhibiting Pulmonary Vascular Remodeling

Rui Wang^{1,2†}, Jinjin Pan^{1†}, Jinzhen Han^{1†}, Miaomiao Gong¹, Liang Liu¹, Yunlong Zhang⁴, Ying Liu⁴, Dingyou Wang¹, Qing Tang¹, Na Wu¹, Lin Wang¹, Jinsong Yan^{2*}, Hua Li^{3*} and Yuhui Yuan^{1*}

¹ The Second Affiliated Hospital, Institute of Cancer Stem Cell, Dalian Medical University, Dalian, China, ² Liaoning Key Laboratory of Hematopoietic Stem Cell Transplantation and Translational Medicine, Liaoning Medical Center for Hematopoietic Stem Cell Transplantation, Dalian Key Laboratory of Hematology, Second Hospital of Dalian Medical University, Dalian, China, ³ College of Pharmacy, Dalian Medical University, Dalian, China, ⁴ The First Affiliated Hospital, Dalian Medical University, Dalian, China

OPEN ACCESS

Edited by:

Andrea Caporali,
University of Edinburgh,
United Kingdom

Reviewed by:

Alejandro Gonzalez-candia,
Institute of Health Sciences, University
O'Higgins, Chile
German Ebersperger,
University of Chile, Chile

*Correspondence:

Yuhui Yuan
yuhuiyuan@hotmail.com
Hua Li
dllihua@126.com
Jinsong Yan
yanjsdmu@dmu.edu.cn

† These authors share first authorship

Specialty section:

This article was submitted to
Cardiovascular Therapeutics,
a section of the journal
Frontiers in Cardiovascular Medicine

Received: 07 October 2021

Accepted: 21 February 2022

Published: 24 March 2022

Citation:

Wang R, Pan J, Han J, Gong M,
Liu L, Zhang Y, Liu Y, Wang D,
Tang Q, Wu N, Wang L, Yan J, Li H
and Yuan Y (2022) Melatonin
Attenuates Dasatinib-Aggravated
Hypoxic Pulmonary Hypertension via
Inhibiting Pulmonary Vascular
Remodeling.
Front. Cardiovasc. Med. 9:790921.
doi: 10.3389/fcvm.2022.790921

Dasatinib treatment is approved as first-line therapy for chronic myeloid leukemia. However, pulmonary hypertension (PH) is a highly morbid and often fatal side-effect of dasatinib, characterized by progressive pulmonary vascular remodeling. Melatonin exerts strong antioxidant capacity against the progression of cardiovascular system diseases. The present work aimed to investigate the effect of melatonin on dasatinib-aggravated hypoxic PH and explore its possible mechanisms. Dasatinib-aggravated rat experimental model of hypoxic PH was established by utilizing dasatinib under hypoxia. The results indicated that melatonin could attenuate dasatinib-aggravated pulmonary pressure and vascular remodeling in rats under hypoxia. Additionally, melatonin attenuated the activity of XO, the content of MDA, the expression of NOX4, and elevated the activity of CAT, GPx, and SOD, the expression of SOD2, which were caused by dasatinib under hypoxia. *In vitro*, dasatinib led to decreased LDH activity and production of NO in human pulmonary microvascular endothelial cells (HPMECs), moreover increased generation of ROS, and expression of NOX4 both in HPMECs and primary rat pulmonary arterial smooth muscle cells (PASMCS) under hypoxia. Dasatinib up-regulated the expression of cleaved caspase-3 and the ratio of apoptotic cells in HPMECs, and also elevated the percentage of S phase and the expression of Cyclin D1 in primary PASMCS under hypoxia. Melatonin ameliorated dasatinib-aggravated oxidative damage and apoptosis in HPMECs, meanwhile reduced oxidative stress level, proliferation, and repressed the stability of HIF1- α protein in PASMCS under hypoxia. In conclusion, melatonin significantly attenuates dasatinib-aggravated hypoxic PH by inhibiting pulmonary vascular remodeling in rats. The possible mechanisms involved protecting endothelial cells and inhibiting abnormal proliferation of smooth muscle cells. Our findings may suggest that melatonin has potential clinical value as a therapeutic approach to alleviate dasatinib-aggravated hypoxic PH.

Keywords: melatonin, dasatinib, pulmonary hypertension, vascular remodeling, hypoxia, oxidative stress

INTRODUCTION

Dasatinib is one kind of second-generation multiple tyrosine kinase inhibitors primarily used to treat patients with chronic myeloid leukemia (CML) and Philadelphia chromosome-positive acute lymphoid leukemia (Ph⁺ ALL). For most CML and Ph⁺ ALL patients, dasatinib has made this potentially devastating disease into a manageable chronic condition. However, pulmonary hypertension (PH) is a recognized side-effect of dasatinib that occurs at any time during the treatment course, ranging from months to over one year (1–3). Although some functional and clinical improvements of patients were observed after cessation of dasatinib, the majority of patients failed to recover completely, and some died of PH-associated cardiac failure or even suffered from sudden death, suggesting that pulmonary vascular remodeling caused by dasatinib is the key clinical issue of dasatinib-associated PH (4, 5).

Pulmonary hypertension is a lethal disease featured by progressive pulmonary vascular remodeling that contributed to the obliteration of distal pulmonary arteries and elevated pulmonary artery pressure, leading to the right ventricle (RV) hypertrophy, eventually to heart failure (1, 6, 7). Pulmonary artery endothelial dysfunction and aberrant smooth muscle cells (SMCs) proliferation are involved in the pathological development of vascular remodeling. Recent studies have demonstrated that the impact of dasatinib on pulmonary endothelial cells (ECs) contributed substantially to PH, mainly through inducing mitochondrial reactive oxygen species (ROS) production, endoplasmic reticulum stress, and ECs apoptosis (8). ROS is able to stabilize hypoxia-inducible factor 1- α (HIF1- α) protein expression (9), HIF-1 α functions as an intrinsic pathogenic determinant in many types of PH, including monocrotaline-induction and genetic forms (10, 11). Whereas, there is limited evidence about HIF-1 α in dasatinib-associated PH and a lack of drugs targeting for pulmonary vascular remodeling of PH in dasatinib-treated patients, and no cure for this devastating disease at present (12, 13). Thereby, it is significant to develop effective drugs for attenuating vascular remodeling against dasatinib-associated PH.

Oxidative stress is regarded to play a crucial role in vascular remodeling of PH (14–17). In this context, natural antioxidants have been used as treatments for PH. Melatonin (N-acetyl-5-methoxytryptamine) is a small lipophilic molecule and ubiquitous physiological mediator mainly synthesized in pineal gland (18). As a neurohormone, melatonin is characterized with pleiotropic activities, such as treating insomnia (19), inhibiting tumor growth (20, 21), and being utilized as an adjuvant of cancer therapies (22, 23). Numerous investigations have indicated that melatonin also has many benefits on the cardiovascular system, including regulation of atherosclerosis, depression of hypertension, and prevention of hypertensive heart disease (24–26). Moreover, melatonin alleviated hemodynamics and pulmonary vascular remodeling in hypoxic PH rats (18), decreased pulmonary vascular remodeling and oxygen sensitivity in pulmonary hypertensive newborn lambs (16), and alleviated vascular disorders in monocrotaline-induced PH rats (27).

Nevertheless, the efficacy of melatonin on dasatinib-associated PH has not been investigated so far.

In the present study, we explored the effect and the possible underlying mechanism of melatonin on dasatinib-aggravated PH. Melatonin treatment blunted pulmonary vascular remodeling and significantly attenuated hemodynamics in a rat model of dasatinib-aggravated PH under normobaric hypoxic condition. *In vitro* findings suggest that melatonin may reduce pulmonary vascular remodeling by protecting ECs and inhibiting proliferation of SMCs.

MATERIALS AND METHODS

Animal Experiments

Adult male Sprague–Dawley (SD) rats (6–8 weeks) weighing from 120 to 150 g were obtained from the Animal Center of Dalian Medical University (Dalian, China). All procedures were carried out following the Institutional Animal Care and Use Committee guidelines, and approved by the Institutional Ethics Committee.

Dasatinib-aggravated experimental model of hypoxic PH was established as previously described (8). Forty-eight adult male SD rats were randomly divided into six groups ($n = 8$): (1) vehicle under normoxia (Nor + Vehicle) group, (2) dasatinib under normoxia (Nor + Das) group, (3) melatonin under normoxia (Nor + Mel) group, (4) vehicle under hypoxia (Hyp + Vehicle) group, (5) dasatinib under hypoxia (Hyp + Das) group, and (6) dasatinib with melatonin administration under hypoxia (Hyp + Das + Mel) group.

Normoxia groups rats were maintained in room air, hypoxia groups rats were kept in chambers for normobaric hypoxia in the same room and had free access to water and regular chow. The oxygen fraction inside the chamber was maintained at 10% flushed with N₂ and room air. The hypoxia groups rats underwent normobaric hypoxic condition (10% O₂, 12 h/day) at day 14 for 3 weeks. Nor + Das group rats were treated with daily i.p. injection of dasatinib (Selleck, United States) at a dose of 10 mg/kg/day for 4 weeks, Hyp + Das and Hyp + Das + Mel group rats were treated with daily i.p. injection of dasatinib for 1 week and received hypoxia induction for the next 3 weeks, Nor + Mel and Hyp + Das + Mel group rats were administrated with daily i.p. injection of melatonin (Sigma, United States) at a dose of 15 mg/kg/day for the entire 5 weeks.

Echocardiography

Cardiopulmonary parameters, including cardiac output and velocity-time integral (VTI) were measured using non-invasive digital ultrasound micro-imaging system (Vevo 770 system VisualSonics, Canada) as previously described (28).

Hemodynamic Experiments

Measurement of right ventricular systolic pressure (RVSP) was performed as described previously (18, 29). Blood samples were obtained from the heart into EDTA tubes (2 mL K⁺/EDTA), centrifuged at 3,000 rpm for 15 min, and plasma was kept at –80°C for subsequent experiments. The RV was separated from

the left ventricle plus septum (LV + S), and the RV/(LV + S) ratio was calculated as the Fulton index. The Fulton index [RV/(LV + S)] and RV/body weight (BW) were calculated as RV hypertrophy. The lung tissues were dissected into 4- μ m-thick slices and placed in 4% paraformaldehyde solution for 72 h. The left lungs were stored at -80°C for subsequent experiments.

Morphological Investigation

The right lungs were fixed in 4% paraformaldehyde buffer at 4°C for 72 h, the midsagittal slices of right lungs were processed for paraffin embedding and sliced into 4- μ m-thick sections. The sections were next subjected to hematoxylin and eosin (HE) staining according to the established techniques (18, 30). The percent medial wall thickness (WT%) = $([2 \times \text{medial wall thickness}/\text{external diameter}] \times 100)$, and percent medial wall area (WA%) = $([\text{medial wall area}/\text{total vessel area}] \times 100)$ were calculated to assess pulmonary vascular structure remodeling.

Pulmonary Immunohistochemistry

Sections were dewaxed, rehydrated, retrieved the antigens, and treated with 1% H_2O_2 for 15 min at room temperature to block endogenous peroxidase. After incubated with 5% bovine serum albumin for 30 min, sections were treated with the primary antibodies against α -SMA (1:1,000, ab7817, Abcam, United States), PCNA (1:5,000, 2586, Cell Signaling Technology, United States) at 4°C overnight. Then, a biotinylated anti-mouse IgG antibody and an avidin-biotinylated peroxidase complex were applied with 3, 3'-diaminobenzidine as a peroxidase substrate. Immunoreactivity was visualized by diaminobenzidine. A light hematoxylin counterstain was applied.

The integrated optical density (OD) of α -SMA was analyzed in the wall of the pulmonary arterioles, and the degree of pulmonary arteries muscularization was also determined by α -SMA staining. As previously described (30), 30–40 arteries were categorized as non-muscularized (α -SMA staining $<25\%$ of vessel circumference), partial muscularized (α -SMA staining 25–74% of circumference), or full muscularized (α -SMA staining $>75\%$ of circumference) vessels in each rat. The percentages of full muscularized vessels were calculated by dividing the number of vessels in the muscularized category by the total number counted in the same experimental group. Additionally, the numbers of PCNA-positive cells and all the cells in the pulmonary arterial media walls were counted. The percentage of PCNA-positive cell number was calculated as positive cells/all cells.

Measurement of Plasma Melatonin Level

The quantitative determination of plasma melatonin concentrations was performed by enzyme-linked immunosorbent assay (E-EL-R0031c, Elabscience, China), according to the manufacturer's guidelines. The lower limit of detection in this assay is 15.63 pg/mL, the intra-assay coefficient of variation (CV) is less than 5.24%, and the inter-assay CV is less than 5.30%.

Rat Primary PSMCs Isolation and Cell Culture

Primary PSMCs were isolated from pulmonary arteries of adult male SD rats (6 weeks old) as previously described (18, 29). Cells from passages 3–6 were used for the *in vitro* studies. Primary PSMCs were cultured in High-glucose DMEM (Gibco, United States) containing 10% (v/v) fetal bovine serum (FBS), and antibiotics (penicillin 100 units/mL, and streptomycin 100 $\mu\text{g}/\text{mL}$).

Human pulmonary microvascular endothelial cells (HPMECs) were obtained from ScienCell. HPMECs were cultured in endothelial cell medium (ECM; ScienCell, United States) containing 10% FBS, endothelial cell growth supplement (ECGS; ScienCell, United States), and antibiotics.

Cell Treatment

HPMECs or PSMCs were divided into six groups: (1) vehicle under normoxia (Nor + Vehicle) group, (2) dasatinib under normoxia (Nor + Das) group, (3) melatonin under normoxia (Nor + Mel) group, (4) vehicle under hypoxia (Hyp + Vehicle) group, (5) dasatinib under hypoxia (Hyp + Das) group, and (6) dasatinib and 10 μM melatonin under hypoxia (Hyp + Das + Mel) group. PSMCs at a density of $4 \times 10^4/\text{mL}$, and HPMECs at a density of $8 \times 10^4/\text{mL}$ were seeded on 96-well plates or culture flask, and treated at the time of 70–75% confluence. Melatonin in FBS-free medium was added 1 h before exposure to 10 nM dasatinib or vehicle under normoxia (21% O_2) or hypoxia (1% O_2) condition for 24 h (18).

Cell Viability Assay

Pulmonary arterial smooth muscle cells at a density of $4 \times 10^4/\text{mL}$, HPMECs at a density of $8 \times 10^4/\text{mL}$ were seeded in 96-well plates, and cell viability was assessed by Cell Counting Kit-8 (CCK-8, Bimake, United States) following the manufacturer's protocol. CCK-8 working solution (10 μL) was added to each well of the plate, and incubated the cells for 2 h in the incubator, then measured the absorbance at 450 nm by a microplate reader.

Intracellular ROS Measurement

Intracellular ROS production was detected using DCFH-DA ROS probes (S0033S, Beyotime, China) (29). Briefly, cells were incubated with the probe (10 μM) for 30 min at 37°C in the dark, then rinsed three times to remove the excess probe and maintained in FBS-free DMEM medium. The fluorescence intensity of DCF was measured by CytoFLEX (Beckman Coulter, United States) in FL-1 channel (FITC).

Apoptosis Assay

Annexin V Apoptosis Detection Kit (556420, BD Biosciences, CA, United States) containing Annexin V-FITC and propidium iodide (PI) was employed to measure the cell apoptosis rate. Measurements of the fluorescence were performed by CytoFLEX (Beckman Coulter, United States).

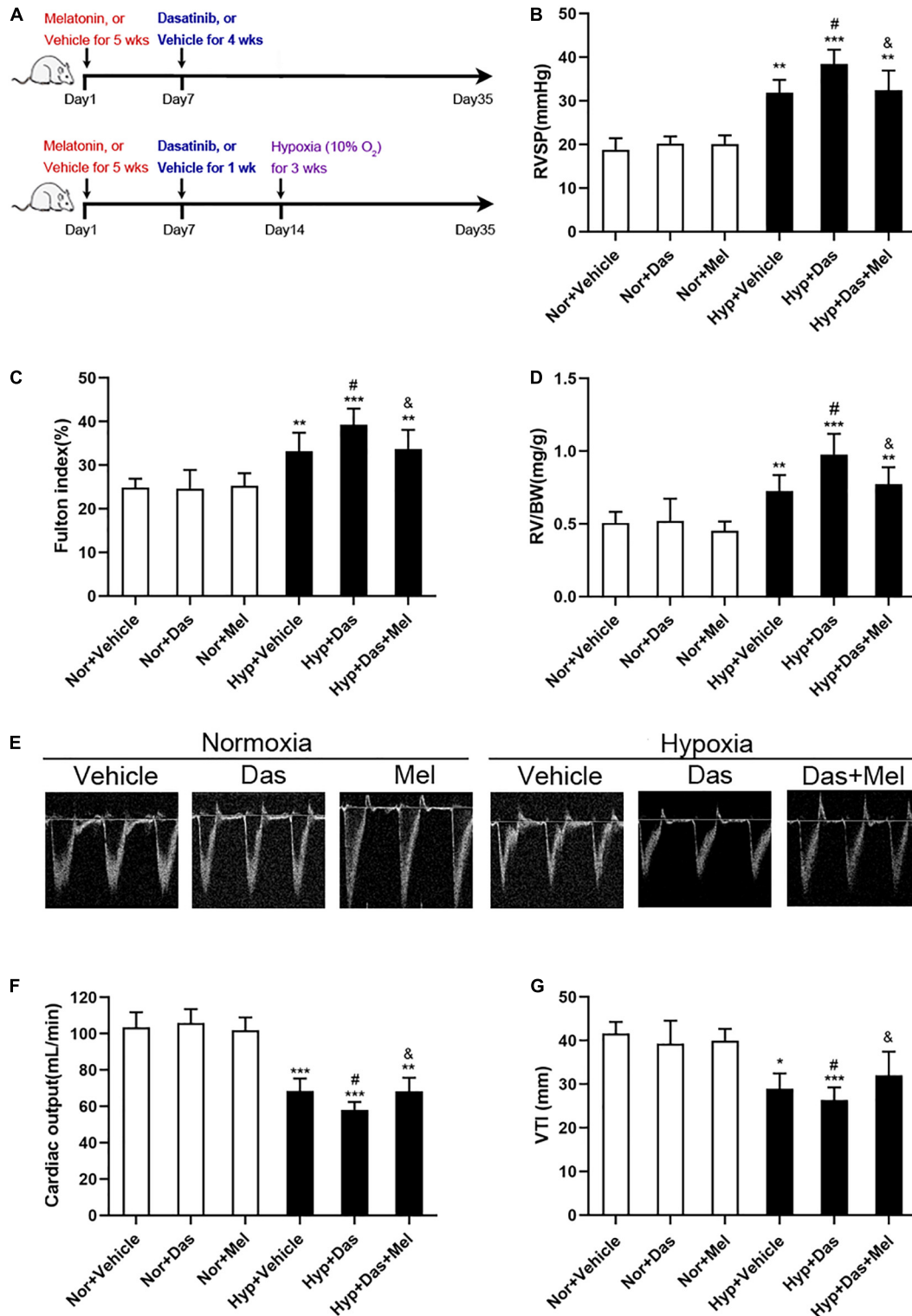
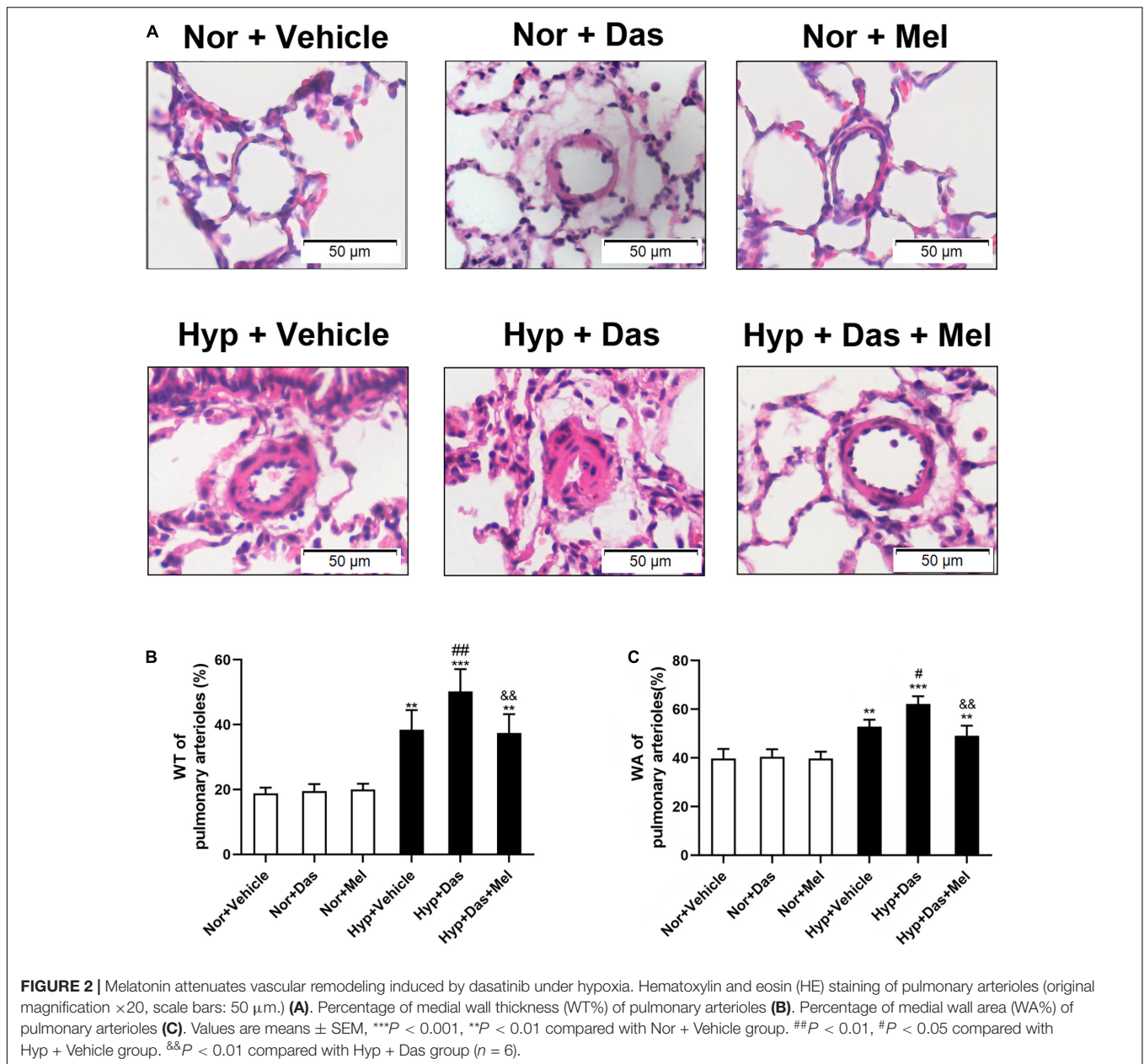


FIGURE 1 | Melatonin attenuates pulmonary hypertension induced by dasatinib under chronic hypoxia. Schematic of rat model used to study the *in vivo* effects of melatonin on pulmonary hypertension induced by dasatinib under hypoxia (A). Values of right ventricular systolic pressure (RVSP) (B), Fulton index (C), RV/BW (D). Echocardiography of right ventricle (E). Values of cardiac output (F) and VTI (G) in melatonin or vehicle pretreated rats which were exposed to dasatinib or vehicle under hypoxia or normoxia. Values are means ± SEM, ****P* < 0.001, ***P* < 0.01, **P* < 0.05 compared with Nor + Vehicle group. #*P* < 0.05 compared with Hyp + Vehicle group. &*P* < 0.05 compared with Hyp + Das group (*n* = 6).



Cell Cycle Assay

The synchronized PASMCS suspension was fixed with cold 75% ethanol at -20°C for 12 h, then stained with PI staining buffer at 37°C for 30 min, and detected by Accuri C6 plus Flow Cytometer (BD Biosciences, San Jose, CA, United States) in FL-2 channel (PE). As described previously (30), further analyses of cell cycle were processed by Flow Jo software.

Xanthine Oxidase, Catalase, and Glutathione Peroxidase Activity Assay

Xanthine oxidase (XO) activity was determined by XO assay kit (BC1095, Solarbio, China), the intra-assay CV is less than 3%, and the inter-assay CV is less than 5%. According to the

manufacturer's instructions, the product of the reaction was quantified at an absorbance of 290 nm.

Catalase (CAT) activity was determined by catalase assay kit (S0051, Beyotime, China), the lower limit of detection in this assay is 1 U/mL, the intra-assay CV is less than 3%, and the inter-assay CV is less than 10%. According to the manufacturer's instructions, the product of the reaction was quantified at an absorbance of 240 nm.

Glutathione peroxidase (GPx) activity was determined by total GPx assay kit with NADPH (S0058, Beyotime, China), the lower limit of detection in this assay is 0.5 mU/mL, the intra-assay CV is less than 3%, and the inter-assay CV is less than 10%. According to the manufacturer's instructions, the product of the reaction was quantified at an absorbance of 340 nm.

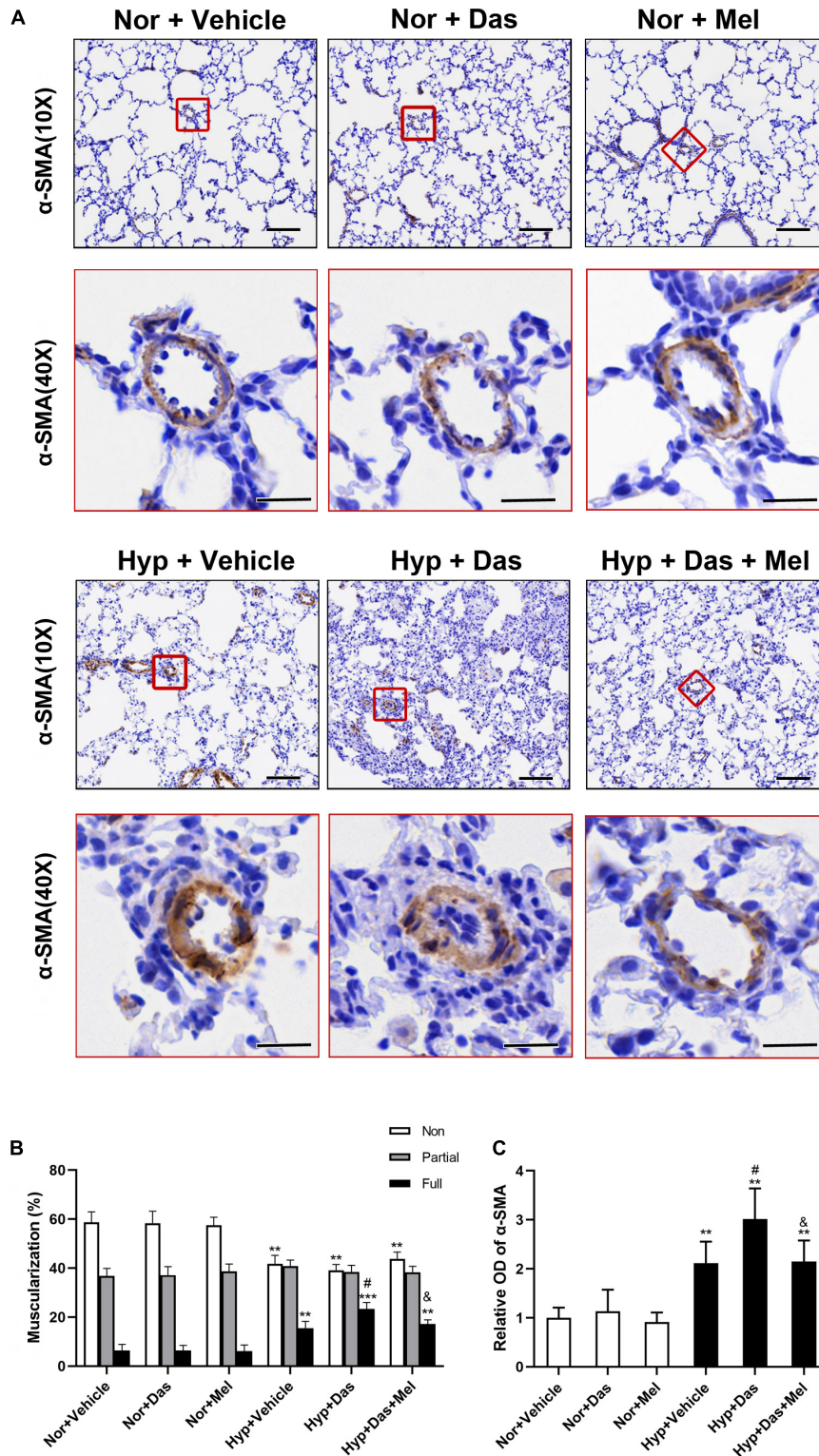
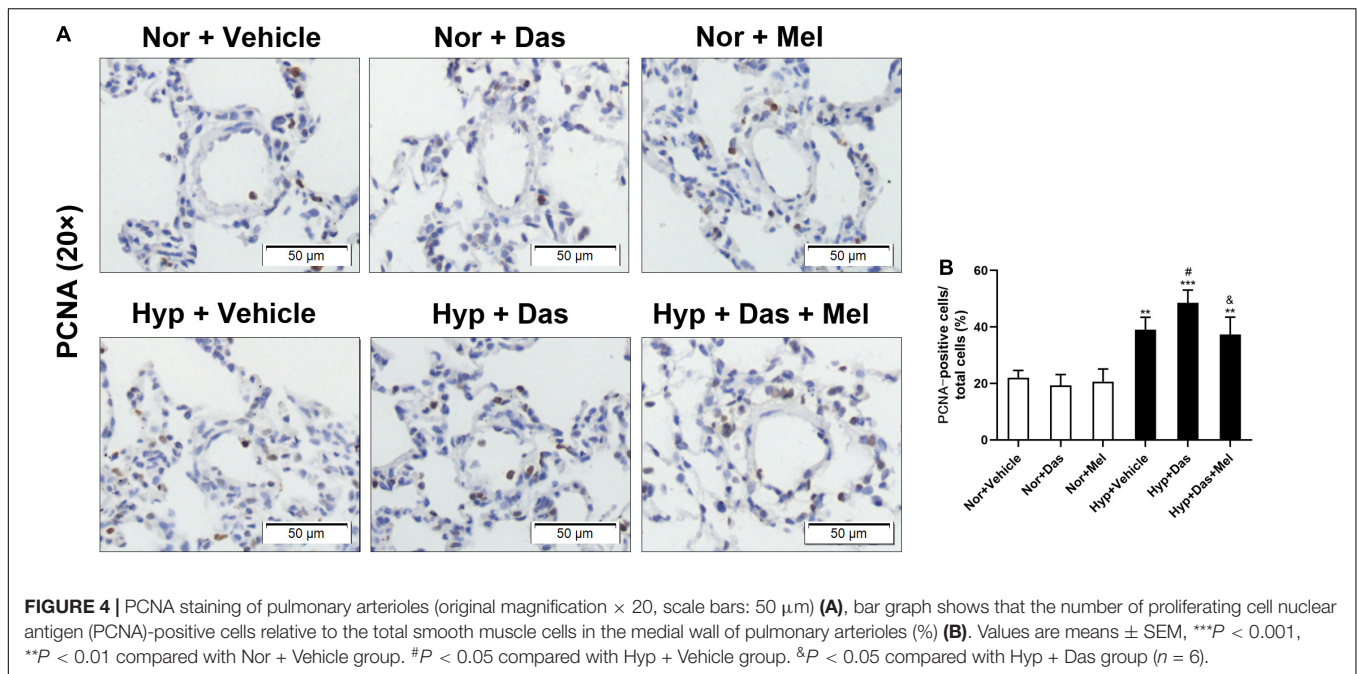


FIGURE 3 | Melatonin attenuates pulmonary arteries muscularization induced by dasatinib under hypoxia. α -SMA (smooth muscle actin) immunohistochemical staining of pulmonary arterioles (original magnification $\times 10$, scale bars: $100\ \mu\text{m}$, and original magnification $\times 40$, scale bars: $20\ \mu\text{m}$) (A). The quantitative analysis of the proportion of muscularized pulmonary arteries (sized $25\text{--}100\ \mu\text{m}$) (B). The quantitative analysis of OD value of α -SMA immunoreactivity in pulmonary arterioles (C). Values are means \pm SEM, $***P < 0.001$, $**P < 0.01$ compared with Nor + Vehicle group. $\#P < 0.05$ compared with Hyp + Vehicle group. $\&P < 0.05$ compared with Hyp + Das group ($n = 6$).



Superoxide Dismutase, Lactate Dehydrogenase Activity, and Malondialdehyde Content Assay

Superoxide dismutase (SOD) activity was determined by SOD activity assay kit (S0101S, Beyotime, China), the lower limit of detection in this assay is 0.5 U/mL, the intra-assay CV is less than 3%, and the inter-assay CV is less than 15%. According to the manufacturer's instructions, the product of the reaction was quantified at an absorbance of 450 nm.

Lactate dehydrogenase (LDH) activity was determined LDH activity assay kit (C0016, Beyotime, China), the lower limit of detection in this assay is 0.65 mU/mL, the intra-assay CV is less than 3%, and the inter-assay CV is less than 10%. According to the manufacturer's recommendations, the product of the reaction was quantified at an absorbance of 490 nm.

Malondialdehyde (MDA) content was determined by Micro-MDA assay kit (KGT003-1, Keygen, China), the lower limit of detection in this assay is 0.5 nmol/mL, the intra-assay CV is less than 2.3%, and the inter-assay CV is less than 5.4%. According to the manufacturer's instructions, the product of the reaction was quantified at an absorbance of 532 nm.

NO Generation Measurement

NO generation was measured using a fluorescence method. In this assay, 3-amino, 4-aminomethyl-2', 7'-difluorescein, diacetate (DAF-FM-DA, S0019, Beyotime, China) was used as a fluorescent indicator of intracellular NO. Briefly, HPMECs were incubated with 5 mM DAF-FM-DA at 37°C for 20 min. Cells were then rinsed three times to remove the excess probe and maintained in phosphate-buffered saline (PBS) throughout the experiments. Fluorescence was recorded at excitation 495 nm/emission 515 nm on a fluorescence multi-well plate reader (Spark, Tecan Trading

AG, Switzerland). Data were expressed as the fluorescence signal of the sample relative to the control.

MitoSOX Red Staining

Pulmonary arterial smooth muscle cells were incubated with 5.0 μM MitoSOX Red Mitochondrial Superoxide Indicator (Yeasen, China) for 15 min to detect mitochondrial superoxide production using a fluorescent microscope (Olympus, Japan).

Western Blotting Analysis

Protein expression in total lung tissues, HPMECs, and PSMCs were determined by Western blotting. After transfection, the PVDF membranes (Millipore, United States) were blocked with 5% skim milk to prevent non-specific binding, then incubated with specific primary antibodies against HIF1- α (1:500, ab216842, Abcam, United States), NOX4 (1:1,000, 14347-1-AP, Proteintech, China), SOD2 (1:1,000, 24127-1-AP, Proteintech, China), SOD1(1:1,000, 10269-1-AP, Proteintech, China), Cleaved Caspase-3 (1:1,000, 9664, Cell Signaling Technology, United States), Bcl-xL (1:1,000, AB126, Beyotime, China), β -actin (1:2,500, 60008-1-Ig, Proteintech, China). After washing with TBST buffer, the membranes were incubated with appropriate secondary antibody conjugated with horseradish peroxidase, and signals were detected using by enhanced chemiluminescent kit (Amersham Biosciences, United Kingdom). The relative OD of Western blotting was calculated with the Image lab software (Bio-Rad Laboratories, Hercules, CA, United States).

Statistical Analyses

The mean values \pm SEM were calculated and plotted using GraphPad Prism 7 software (GraphPad Software, San Diego, CA, United States). Differences between multiple groups with one variable were determined using by one-way ANOVA followed

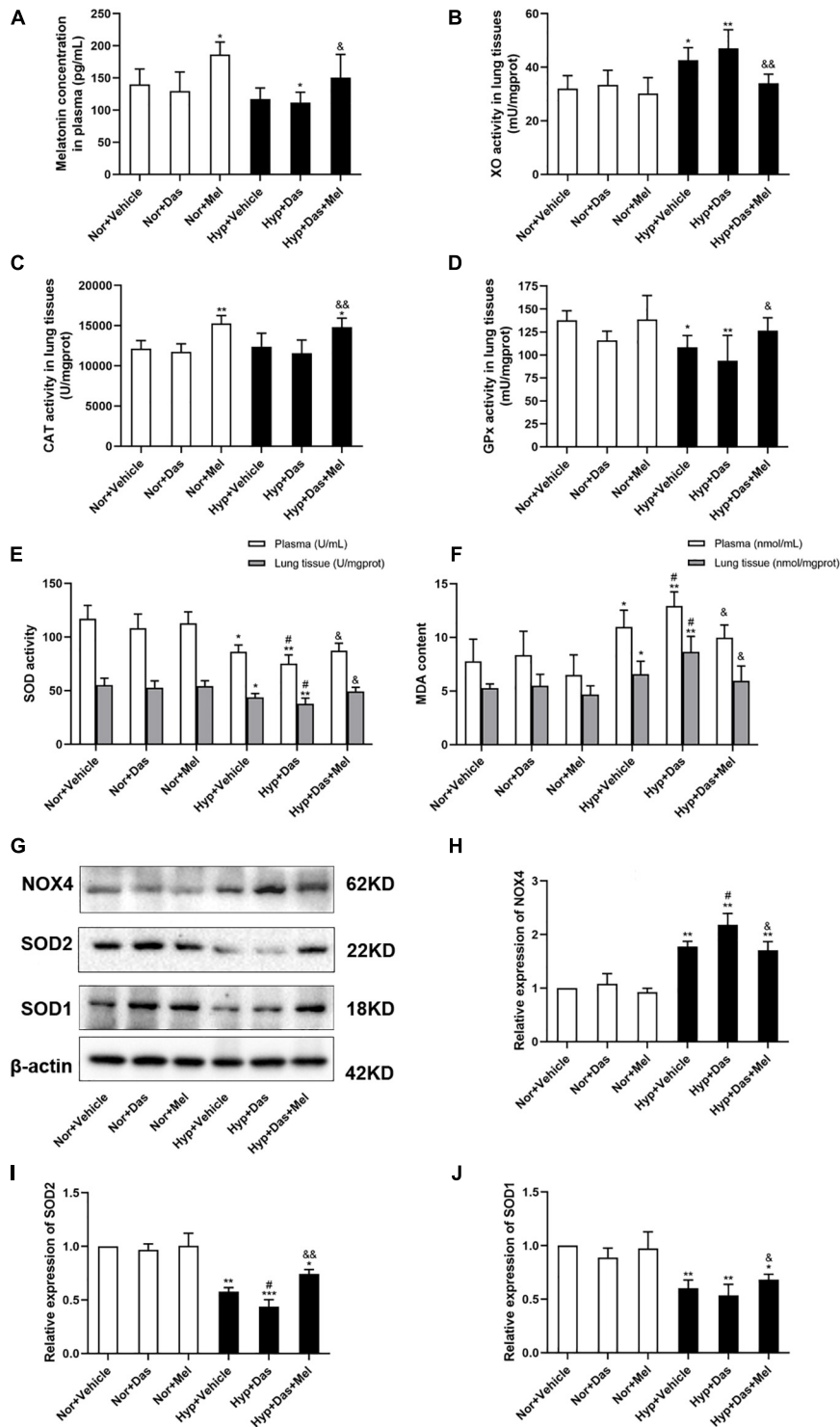


FIGURE 5 | Melatonin attenuates pulmonary oxidative stress induced by dasatinib under hypoxia. The melatonin concentration in rat plasma (A), xanthine oxidase (XO) activity in rat lung tissues (B), Catalase (CAT) activity in rat lung tissues (C), Glutathione peroxidase (GPx) activity in rat lung tissues (D) (n = 6). The activity of superoxide dismutase (SOD) in rat plasma and lung tissues (E), Malondialdehyde (MDA) content in plasma and rat lung tissues (F) (n = 6). Protein expression of NOX4, SOD2, and SOD1 in rat lung tissues (G). Bar graph shows the statistic results of NOX4 (H), SOD2 (I), and SOD1 (J) protein levels (n = 3). Values are means ± SEM, ***P < 0.001, **P < 0.01, *P < 0.05 compared with Nor + Vehicle group. #P < 0.05 compared with Hyp + Vehicle group. &&P < 0.01, &P < 0.05 compared with Hyp + Das group.

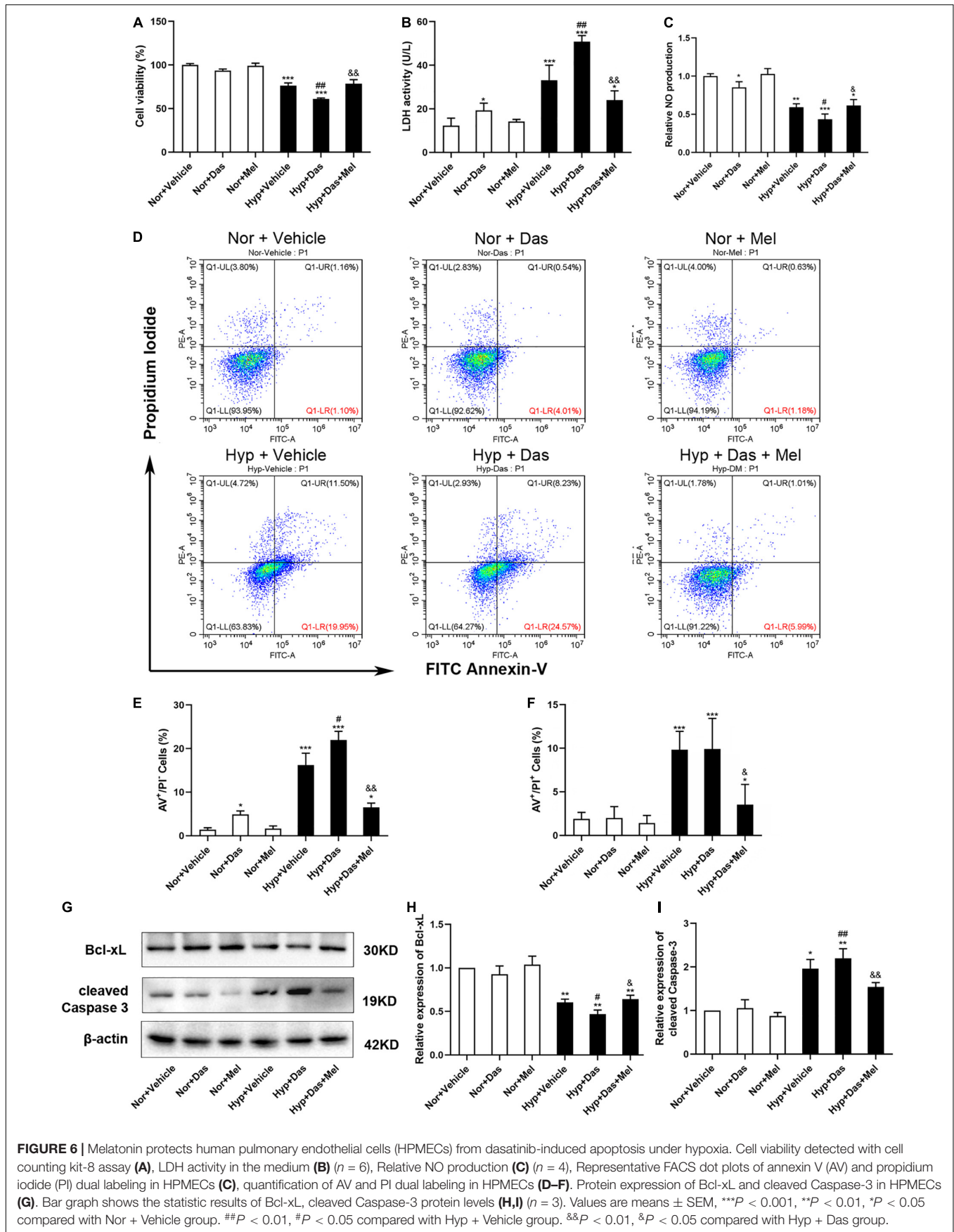
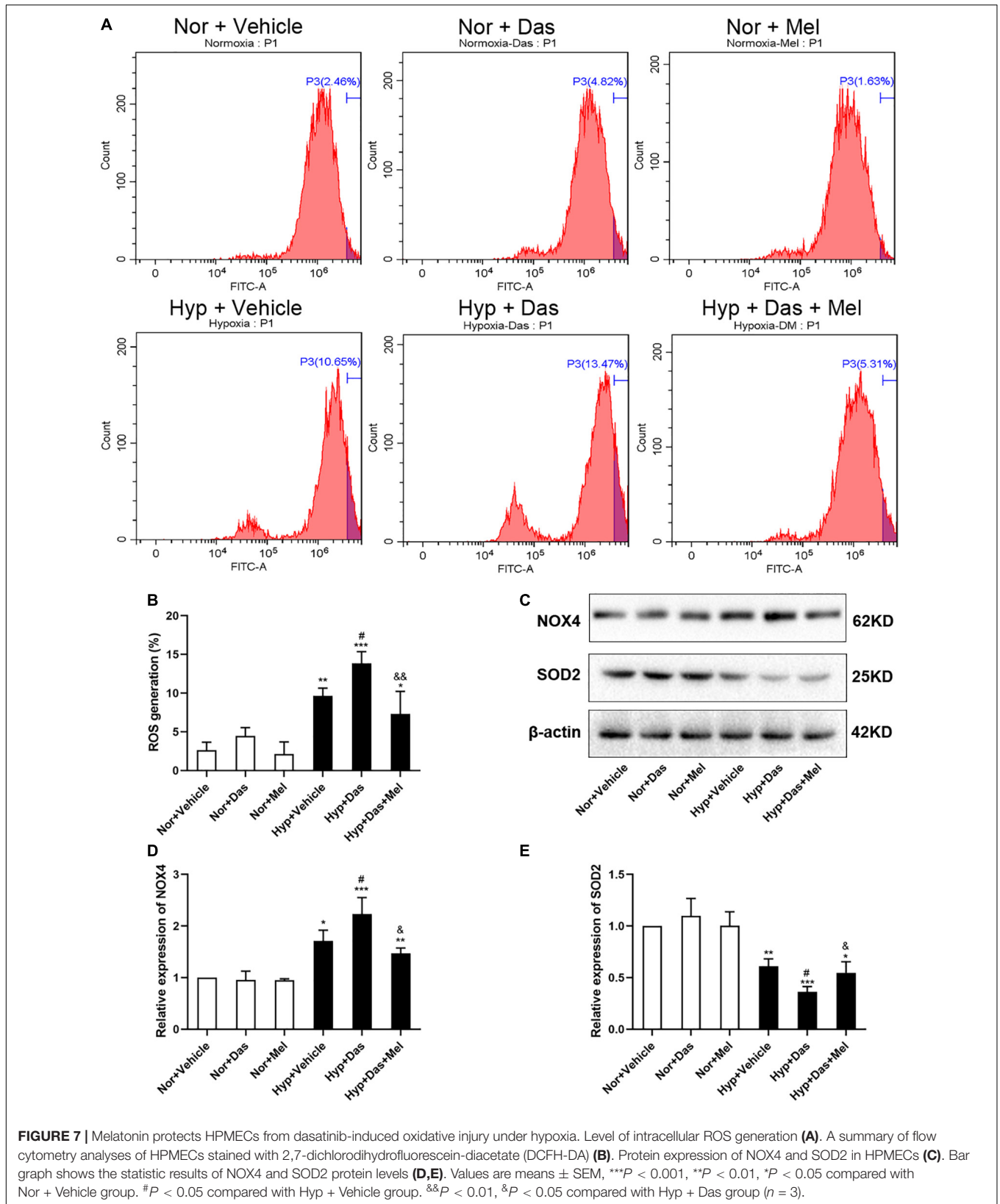


FIGURE 6 | Melatonin protects human pulmonary endothelial cells (HPMECs) from dasatinib-induced apoptosis under hypoxia. Cell viability detected with cell counting kit-8 assay (A), LDH activity in the medium (B) (n = 6), Relative NO production (C) (n = 4), Representative FACS dot plots of annexin V (AV) and propidium iodide (PI) dual labeling in HPMECs (C), quantification of AV and PI dual labeling in HPMECs (D–F). Protein expression of Bcl-xL and cleaved Caspase-3 in HPMECs (G). Bar graph shows the statistic results of Bcl-xL, cleaved Caspase-3 protein levels (H,I) (n = 3). Values are means ± SEM, ***P < 0.001, **P < 0.01, *P < 0.05 compared with Nor + Vehicle group. ##P < 0.01, #P < 0.05 compared with Hyp + Vehicle group. &&P < 0.01, &P < 0.05 compared with Hyp + Das group.



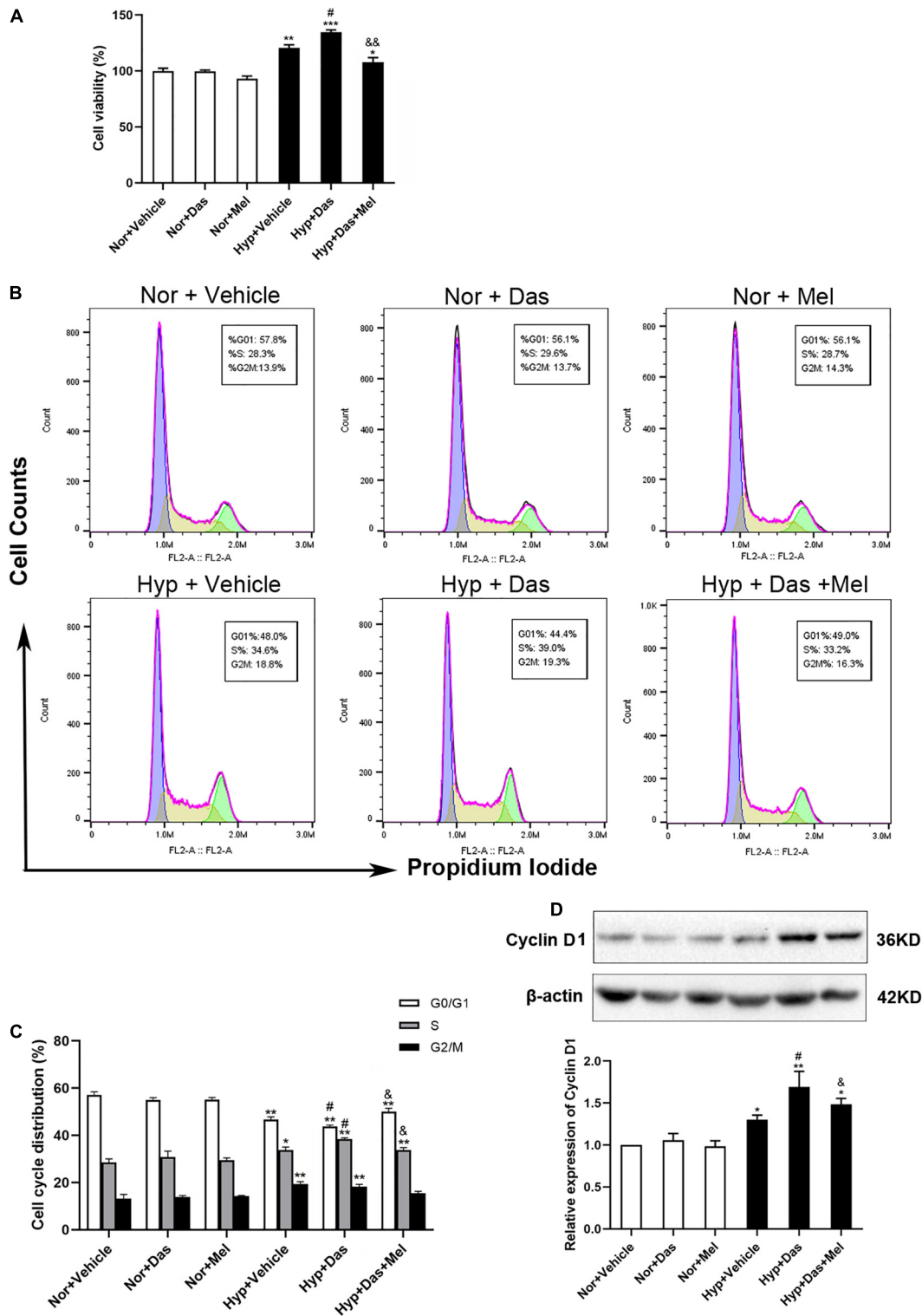


FIGURE 8 | Melatonin arrests cell cycle process acceleration of pulmonary artery smooth muscle cells (PASCs) induced by dasatinib under hypoxia. Viability of PASCs pretreatment with melatonin or vehicle induced by dasatinib under hypoxia for 24 h was determined by cell counting kit-8 (CCK8) assay (A). Representative FACS dot plots of cell cycle in PASCs (B), the percentage of cells at each phase of cell cycle was quantified (C). Protein expression of Cyclin D1 in PASCs (D). Values are means \pm SEM, *** $P < 0.001$, ** $P < 0.01$, * $P < 0.05$ compared with Nor + Vehicle group. # $P < 0.05$ compared with Hyp + Vehicle group. && $P < 0.01$, & $P < 0.05$ compared with Hyp + Das group ($n = 3$).

by Bonferroni's *post hoc* test. To compare multiple groups with more than one variable were determined using two-way ANOVA followed by Bonferroni's *post hoc* test was used. Significant difference was accepted at $P < 0.05$.

RESULTS

Melatonin Attenuated Dasatinib-Aggravated Hypoxic Pulmonary Hypertension in Rats

To investigate the *in vivo* effects of melatonin on dasatinib-associated PH. Firstly, we established the dasatinib-aggravated experimental model of hypoxic PH (8). SD rats were treated with daily i.p. injection of dasatinib (10 mg/kg) or vehicle at day 7 for 1 week or 4 weeks, then administrated for PH induction: under chronic normobaric hypoxic condition (10% O₂, 12 h/day) treatment (Hypoxia) for 3 weeks (as previously described). Before the establishment of dasatinib-aggravated PH model, rats were received daily i.p. injection of melatonin (15 mg/kg) for the entire 5 weeks (Figure 1A).

We found an increase in hemodynamics (right ventricle systolic pressure, RVSP) in Hyp + Das group rats (Figure 1B). In accordance with the RVSP, severer right ventricular hypertrophy (Fulton index, and RV/BW) (Figures 1C,D), lower cardiac output (Figure 1F) and VTI (Figure 1G) in Hyp + Das group, compared to Hyp + Vehicle group rats. While the RVSP, Fulton index, RV/BW, cardiac output, and VTI in Hyp + Das + Mel group was reversed in the Hyp + Das + Mel group (Figures 1B–G).

Melatonin Reduced Dasatinib-Aggravated Pulmonary Vascular Remodeling Under Hypoxia in Rats

We next investigated the effects of melatonin on dasatinib-aggravated pulmonary artery remodeling in rats. The histological analyses showed that dasatinib produced a promotable effect on wall thickness (WT%) and wall area (WA%) of small pulmonary arteries in PH rats, while the WT% and WA% of Hyp + Das + Mel group rats were much lower than that of Hyp + Das group rats (Figures 2A–C).

Similarly to the observed histological changes, non-and full muscularization vessels showed significant differences between normoxic and hypoxic groups. Also, the percentage of lung full muscularization arterioles in Hyp + Das group rats was higher than that in Hyp + Vehicle group rats. However, the percentage of lung full muscularization arterioles in Hyp + Das + Mel group rats was lower than that in Hyp + Das group rats (Figures 3A,B). α -SMA positive-area of pulmonary arterioles was significantly increased in Hyp + Das group rats, whereas this increment of the α -SMA positive area was lower in Hyp + Das + Mel group rats (Figures 3A,C).

Additionally, we analyzed the cell proliferation in the medial wall of small pulmonary vessels. As Figure 4 showed that the percentage of PCNA-positive cells in Hyp + Das group was higher

than that in Hyp + Vehicle group, the increased cell proliferation was diminished in Hyp + Das + Mel group rats (Figures 4A,B).

Melatonin Ameliorated Dasatinib-Aggravated Pulmonary Oxidative Damage Under Hypoxia in Rats

The melatonin concentration in plasma of Hyp + Das group was lower compared to Nor + Vehicle group, however the melatonin concentration in plasma of Hyp + Das + Mel group was markedly increased, relative to Hyp + Das group (Figure 5A).

Pro-oxidant enzyme XO plays a critical role in the regulation of the oxidant levels in the vasculature of PH. To determine the anti-oxidative effect of melatonin, XO activity in lung tissues was analyzed. Results showed that pulmonary XO activity of Hyp + Das group and Hyp + Vehicle group was higher compared to Nor + Vehicle, melatonin treatment reduced the levels of XO in lung tissues (Figure 5B).

The dysregulation of antioxidant enzymes implicated in the etiology of PH, therefore, the activity of CAT, GPx, and SOD were detected. The CAT activity in lung tissues of Nor + Mel group and Hyp + Das + Mel group was higher compared to Nor + Vehicle group (Figure 5C). Pulmonary GPx activity in Hyp + Vehicle group and Hyp + Das group was lower compared to Nor + Vehicle, melatonin treatment reversed the levels of GPx in lung tissues (Figure 5D). Plasma and pulmonary SOD activity in Hyp + Das group rats were lower compared to Hyp + Vehicle (Figure 5E). However, these above changes were reversed in Hyp + Das + Mel group rats (Figures 5C–E).

MDA is formed as an end product of lipid peroxidation and acts as a marker of endogenous lipid peroxidation. Our results showed that plasma and pulmonary MDA content in Hyp + Das group rats were higher compared to Hyp + Vehicle group, these changes were inhibited in Hyp + Das + Mel group rats (Figure 5F).

Furthermore, as Figures 5G–J shown that pulmonary SOD2 expression in Hyp + Das group rats was lower compared to Hyp + Vehicle group, NOX4 expression was higher than Hyp + Vehicle group, but SOD1 expression showed no significant change between Hyp + Das group and Hyp + Vehicle group. The above changes were reversed by melatonin treatment.

Melatonin Protected Human Pulmonary Endothelial Cells (HPMECs) From Dasatinib-Induced Apoptosis via Reducing ROS Production Under Hypoxia

We next assessed that melatonin attenuated pulmonary EC dysfunction which induced by dasatinib under hypoxia via studying its direct effect on HPMECs *in vitro*. The cell viability of HPMECs in Hyp + Das group was diminished than Hyp + Vehicle group, 10 μ M melatonin significantly enhanced HPMEC viability effectively under dasatinib treatment and hypoxia (Figure 6A). LDH activity of HPMEC medium was higher in Hyp + Das group than Hyp + Vehicle group (Figure 6B). NO generation of HPMECs in Hyp + Das

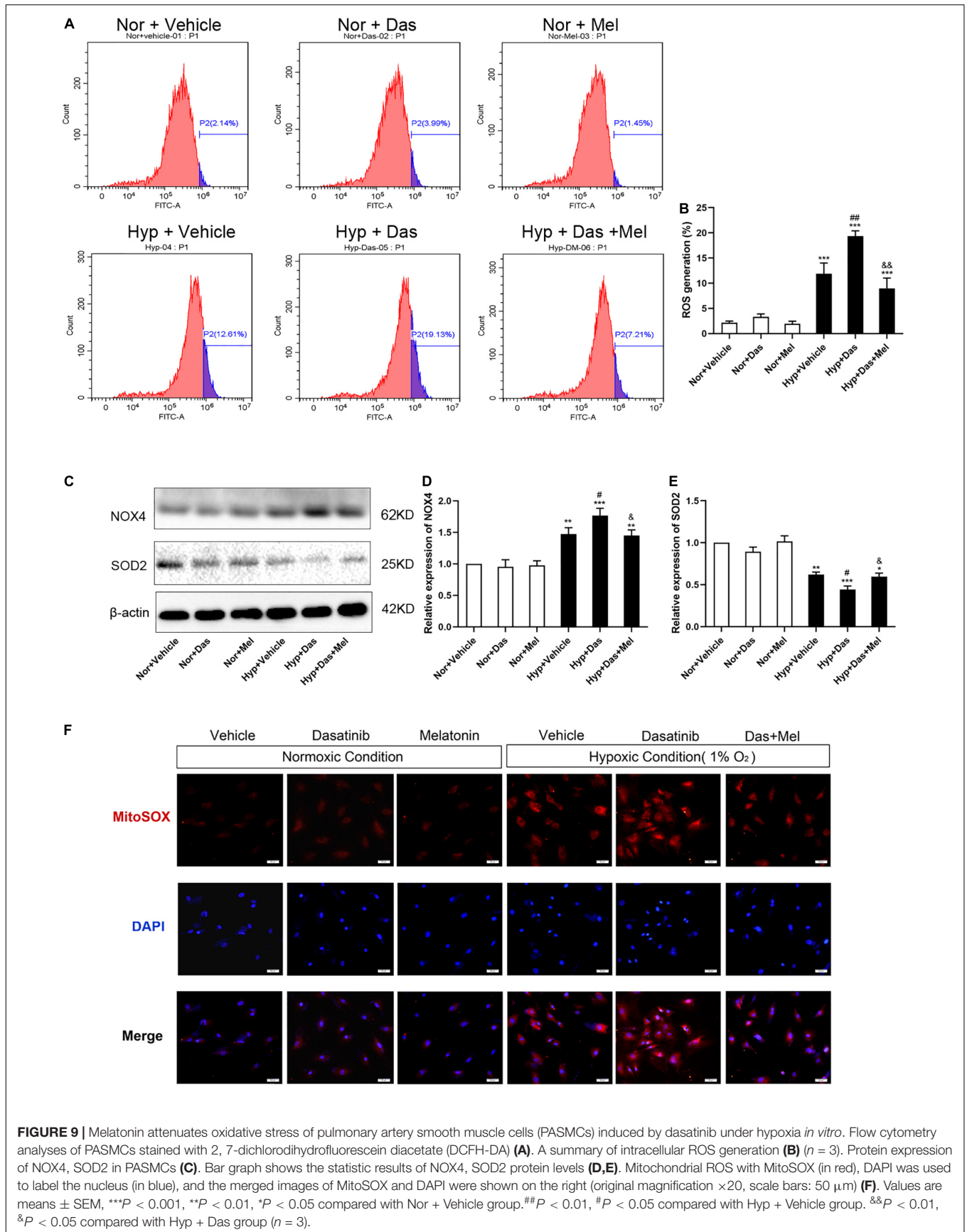


FIGURE 9 | Melatonin attenuates oxidative stress of pulmonary artery smooth muscle cells (PASMCs) induced by dasatinib under hypoxia *in vitro*. Flow cytometry analyses of PASMCs stained with 2, 7-dichlorodihydrofluorescein diacetate (DCFH-DA) (A). A summary of intracellular ROS generation (B) (*n* = 3). Protein expression of NOX4, SOD2 in PASMCs (C). Bar graph shows the statistic results of NOX4, SOD2 protein levels (D,E). Mitochondrial ROS with MitoSOX (in red), DAPI was used to label the nucleus (in blue), and the merged images of MitoSOX and DAPI were shown on the right (original magnification ×20, scale bars: 50 μm) (F). Values are means ± SEM, ****P* < 0.001, ***P* < 0.01, **P* < 0.05 compared with Nor + Vehicle group. ##*P* < 0.01, #*P* < 0.05 compared with Hyp + Vehicle group. &&*P* < 0.01, &*P* < 0.05 compared with Hyp + Das group (*n* = 3).

group was decreased compared to Hyp + Vehicle group, whereas melatonin attenuated the change (Figure 6C). AV-positive/PI-negative cells were elevated in the Hyp + Das group, whereas melatonin attenuated dasatinib- and hypoxia- induced apoptosis of HPMECs and protected endothelial cells from apoptosis in response to injury (Figures 6D–F). Cleaved caspase-3 expression was higher, and Bcl-xL expression was lower in Hyp + Das group than Hyp + Vehicle group, melatonin treatment conspicuously reversed the above-mentioned changes of HPMECs (Figures 6G–I).

To further explore the possible underlying mechanism, we examined oxidative stress level in HPMECs. ROS generation of HPMECs was higher in Hyp + Das group than Hyp + Vehicle group (Figures 7A,B). NOX4 protein expression was higher in Hyp + Das group than Hyp + Vehicle group (Figures 7C,D). Protein expression of SOD2 was lower in Hyp + Das group than Hyp + Vehicle group (Figures 7C,E). Melatonin treatment significantly inhibited the above-mentioned changes of HPMECs (Figure 7).

Melatonin Inhibited Rat PSMCs Proliferation Induced by Dasatinib Under Hypoxia via Reducing ROS Production

Excessive PSMCs proliferation is considered a hallmark of pulmonary vascular remodeling in PH. Hence we detected the role of dasatinib on PSMCs *in vitro*. First, we isolated the PSMCs from rats. Then we investigated the cell viability of PSMCs induced by dasatinib under normoxia or hypoxia. CCK-8 assay showed dasatinib under hypoxia significantly increased the cell viability compared to hypoxia alone, 10 μ M melatonin treatment effectively inhibited the proliferation of PSMCs induced by dasatinib under hypoxia (Figure 8A).

Next, we determined whether the inhibition of dasatinib-aggravated PSMCs proliferation by melatonin was correlated with cell cycle arrest. Dasatinib- and hypoxia-treatment increased the percentage of PSMCs in the S phase with a concomitant decrease in the G0/G1 phase and G2/M phase, whereas melatonin reversed the above-mentioned changes (Figures 8B,C). Additionally, we detected the expression of cyclin D1, the pivotal protein of cell cycle in PSMCs. Cyclin D1 expression was higher in Hyp + Das group than Hyp + Vehicle group PSMCs, however, melatonin remarkably decreased the expression of cyclin D1, which was induced by dasatinib under hypoxia (Figure 8D).

To gain more insight into cellular and molecular mechanisms underlying dasatinib-aggravated PSMCs proliferation, the impact of melatonin on oxidative stress of primary rat PSMCs was assessed. ROS generation and NOX4 expression were higher in Hyp + Das group than Hyp + Vehicle group PSMCs (Figures 9A–D). Protein expression of SOD2 was lower in Hyp + Das group PSMCs than Hyp + Vehicle group PSMCs (Figures 9C,E). Melatonin treatment significantly inhibited above-mentioned changes of PSMCs (Figures 9A–E). Except for NADPH oxidase, mitochondrial ROS is another crucial element that leads to oxidative stress (31–33). Similarly to the protein expression of SOD2 change, dasatinib *in vitro*

treatment under hypoxia led to an increase in mitochondrial ROS production, melatonin reversed the increase in dasatinib-aggravated mitochondrial ROS production of PSMCs under hypoxia (Figure 9F).

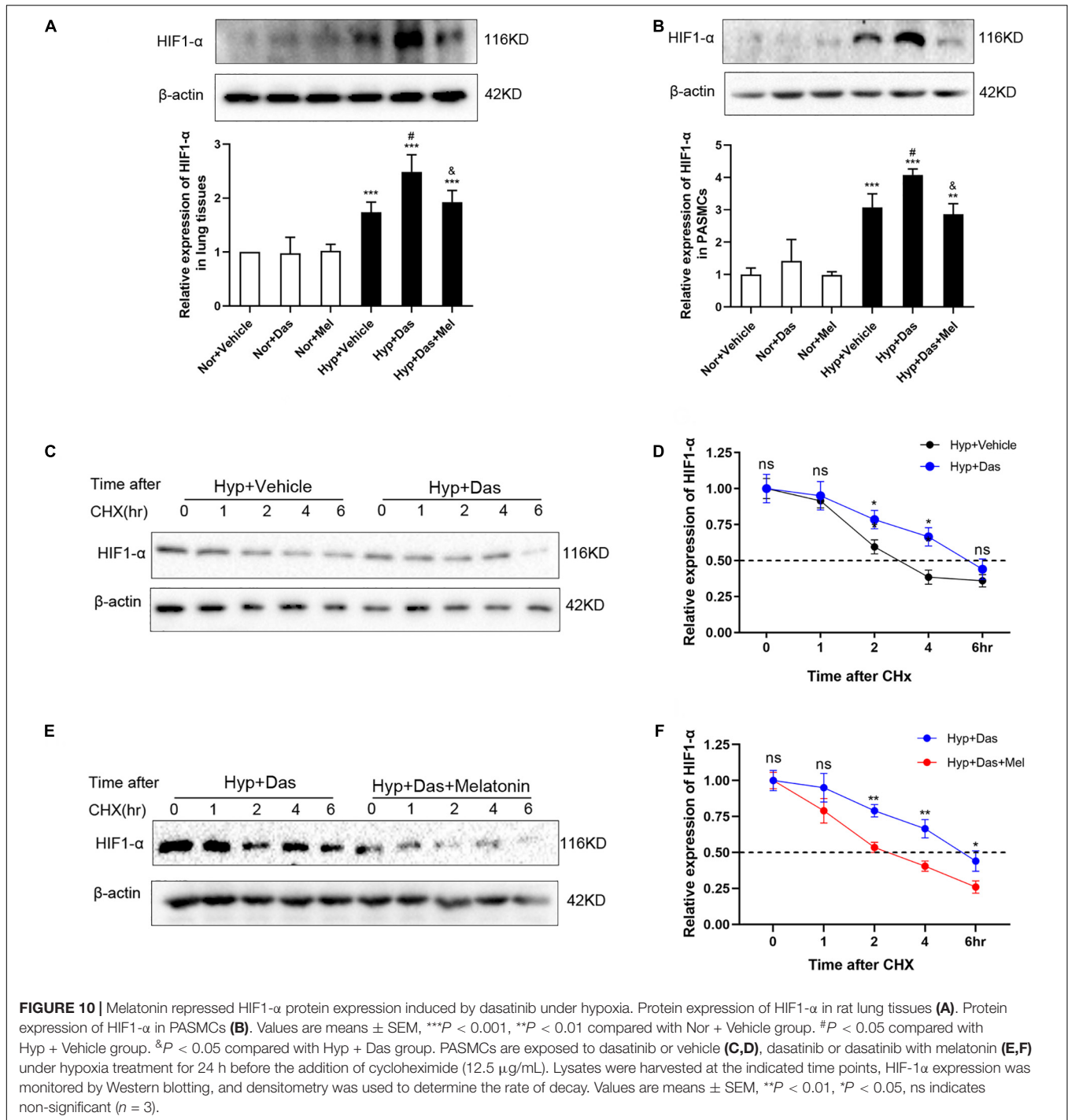
Melatonin Reversed HIF1- α Overexpression and Repressed HIF1- α Protein Stability Induced by Dasatinib Under Hypoxia

HIF1- α (hypoxia-inducible factor 1- α) plays an essential role in the development of pulmonary vascular remodeling during PH (9, 34, 35). Results showed that HIF1- α was higher in Hyp + Das group than Hyp + Vehicle group, and melatonin reversed the dasatinib- and hypoxia-induced up-regulation of HIF1- α both in lungs of rats and PSMCs (Figures 10A,B). Next, we examined whether melatonin influenced the protein stability of HIF1- α with the treatment of dasatinib under hypoxia. As shown in Figures 10C–F, by using cycloheximide (CHx), we found that melatonin repressed HIF1- α protein stability in PSMCs with dasatinib treatment under hypoxia.

DISCUSSION

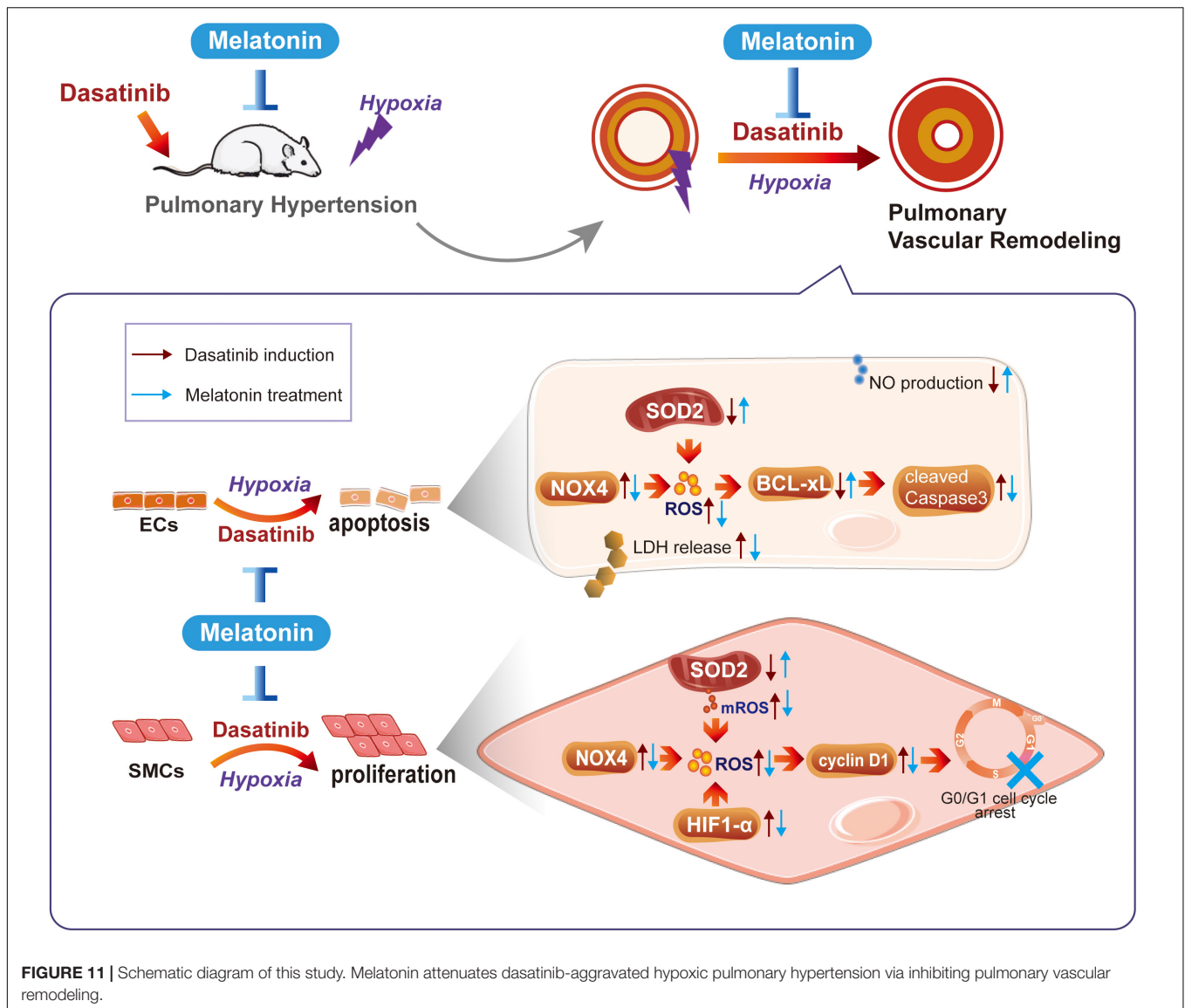
In the present study, the dasatinib-aggravated hypoxic PH model exhibited significant structural remodeling of small pulmonary vessels and elevated RVSP as in the previous report (8), suggested that dasatinib caused the development of PH may through suffering the “second hit” (such as environmental and/or genetic factors). Additionally, dasatinib could induce ECs apoptosis, also cause SMCs proliferation *in vitro*. Notably, melatonin supplementation inhibited dasatinib-aggravated elevation of RVSP, Fulton index, cardio output, WT% and WA% under hypoxia *in vivo*, prevented pulmonary ECs damage, and SMCs proliferation from the induction of dasatinib, suggesting that melatonin attenuated dasatinib-aggravated hypoxic PH in rats.

Obtaining a more comprehensive understanding of the redox pathways and the mechanisms of pro-oxidants/anti-oxidants is significant to develop drugs to prevent vascular remodeling in PH (14–17). It is important to explore the imbalance of anti-oxidases/pro-oxidases in dasatinib-associated PH. CAT, GPx, and SOD are generally considered to be the dominant hydrogen peroxide-scavenging enzymes in the lung. GPx can also act on peroxides other than H₂O₂, such as promoting the reduction of fatty acid hydroperoxides (17, 36, 37). Particularly SOD is the only enzymatic system decomposing superoxide radicals to hydrogen peroxide. SOD serves to catalyze the rapid conversion of superoxide radical to hydrogen peroxide, balances oxygen radicals, and removes stress from oxidation state (38). It has been known that SOD2 protein expression decreases in lung tissues of severe PH patients (39). SOD2 deficiency initiates PH by impairing redox signaling, activating HIF1- α and creating proliferative PSMCs (40). In the present study, dasatinib inhibited SOD and GPx activity, SOD2 expression in rat lungs under hypoxia, while melatonin reversed the above changes induced by dasatinib.



Furthermore, XO is the enzyme that catalyzes the conversion of hypoxanthine to xanthine and xanthine to uric acid with concomitant generation of anion superoxide. Previous studies have shown that the treatment of melatonin did not affect the protein expression of XO in PH newborn sheep, but decreased the activity of XO (41). One mechanism by which oxidants may cause pulmonary injury is lipid peroxidation. MDA level is elevated in serum and plasma of PH patients (42, 43).

NOX4, an essential source of intracellular ROS production, is thought to play a vital role in developing elevated pulmonary artery resistance and pressure (28, 29, 44–47). Our results showed that melatonin attenuated XO activity, MDA content, NOX4 protein expression induced by dasatinib under hypoxia. Together, these observations suggested that melatonin abrogated dasatinib-aggravated pulmonary vascular remodeling through inhibiting pulmonary oxidative stress in rats.



Endothelial dysfunction plays an important role in the initiation and progression of pulmonary vascular remodeling in PH, irrespective of disease origin (48, 49). Pulmonary artery ECs in an apoptotic state liberate a variety of cytokines and ROS, excessively consume NO, which subsequently stimulate endothelial dysfunction (8, 50). Increased level of ROS and apoptosis has been proved to be closely associated to oxidative stress, which is a key factor contributing to pulmonary vascular remodeling. In the present study, melatonin protected HPMECs from dasatinib-induced apoptosis and reduced oxidative stress level via elevating SOD2 expression, diminishing NOX4 expression, and inhibiting ROS generation under hypoxia. The above results suggested that melatonin alleviated dasatinib-aggravated pulmonary vascular remodeling via up-regulating anti-oxidant enzyme, reducing pro-oxidant level, improving NO production and ROS clearance, ameliorating oxidative damage, and inhibiting apoptosis in ECs.

Abnormal proliferation of SMCs is considered a major mechanism underlying the development of pulmonary vascular remodeling in PH. Even if the current medications of PH predominantly targeting vasoconstriction can provide symptomatic relief, they are unable to attenuate excessive PSMCs proliferation and occlusive vascular remodeling (51–54). In the present study, we found that melatonin significantly attenuated the enhanced α -SMA immunoreactivity, the increased full muscularization arterioles, and the elevated PCNA-positive cells of pulmonary arteries induced by dasatinib under hypoxia *in vivo*, suggesting that melatonin remarkably blunted the progressive media thickening induced by dasatinib under hypoxia. It has been reported that dasatinib induces vascular remodeling, involving the progressive thickening of small pulmonary arteries (8). Nevertheless, there is no study about the effect of dasatinib on proliferation of SMCs in PH. Herein, it was found that dasatinib could directly induce PSMCs

proliferation via increasing cell viability and arresting cell cycle process. As one of the key regulators for G1/S transition in the cell cycle, cyclin D1 is up-regulated in excessively proliferative PSMCs by hypoxia, resulting in pulmonary vascular remodeling and PH (55, 56). Notably, our results indicated that melatonin reversed the up-regulation of cyclin D1 and led to cell cycle G0/G1 phase arrest induced by dasatinib under hypoxia in primary rat PSMCs. Furthermore, melatonin mitigated ROS and mitoSOX generation, in accord with NOX4 down-regulation and SOD2 up-regulation under dasatinib- and hypoxia- induction. It has been confirmed that ROS promotes SMCs proliferation both directly and indirectly by inducing auto/paracrine growth mechanisms (57, 58). Taken together, the current results suggested that melatonin mitigated dasatinib-aggravated PSMCs proliferation via promoting the anti-oxidant capacity and scavenging free radicals.

HIF1- α protein expression can be stabilized by ROS (9, 16), the stability of HIF1- α is considered an intrinsic pathogenic determinant in PH (9, 59). SMC-specific *HIF1- α* knockout mice exert less pulmonary vascular remodeling and PH after chronic hypoxia induction (11). Recent studies have implicated that aberrant activation of HIF1- α contributes to PSMCs proliferation, pulmonary vascular remodeling and PH pathogenesis (30, 60). The present study demonstrated that melatonin repressed dasatinib-induced HIF1- α protein stability in primary rat PSMCs under hypoxia. Further studies may focus on the exact mechanism of melatonin on protein stability of HIF1- α in dasatinib-induced PSMCs. The effect of melatonin on ubiquitination and degradation of HIF1- α , regulating HRE sites and revealing associated target genes may be involved in, which were induced by dasatinib is required to be researched.

One of the limitations of our study is that we do not actually know if the effects of melatonin are receptor-mediated. MT1 and MT2 receptors are present in pulmonary vessels of animals (61, 62). Previous study has shown that the MT1 receptor is suggested to be playing a role in the gene regulatory action by melatonin, the MT2 receptor is reported to be involved in mediating vasorelaxation (63). Hence, whether the effects of

melatonin are via receptor dependent or independent mechanism is needed to be explored.

In conclusion, melatonin significantly attenuates dasatinib-induced PH by inhibiting pulmonary vascular remodeling in rats. The mechanisms probably involved protecting ECs through inhibiting oxidative damage and apoptosis, and inhibiting abnormal proliferation of SMCs through decreasing HIF1- α protein stability, oxidative stress, and arresting cell cycle (Figure 11). Our findings may suggest that melatonin has potential clinical value as a therapeutic approach to alleviate dasatinib-aggravated hypoxic PH.

DATA AVAILABILITY STATEMENT

The original contributions presented in the study are included in the article, further inquiries can be directed to the corresponding authors.

ETHICS STATEMENT

The animal study was reviewed and approved by Animal Experimental Ethics Committee of Dalian Medical University.

AUTHOR CONTRIBUTIONS

RW, JH, JY, HL, and YY conceived and designed the experiments. RW, JH, MG, LL, YZ, YL, DW, QT, NW, and LW collected, analyzed, and interpreted the experimental data. RW and JP drafted the manuscript. All authors revised the manuscript critically and approved the final version.

FUNDING

This work was financially supported by the National Natural Science Foundation of China (Nos. 81472492 and 81570124).

REFERENCES

- Montani D, Bergot E, Gunther S, Savale L, Bergeron A, Bourdin A, et al. Pulmonary arterial hypertension in patients treated by dasatinib. *Circulation*. (2012) 125:2128–37. doi: 10.1161/CIRCULATIONAHA.111.079921
- Shah NP, Wallis N, Farber HW, Mauro MJ, Wolf RA, Mattei D, et al. Clinical features of pulmonary arterial hypertension in patients receiving dasatinib. *Am J Hematol*. (2015) 90:1060–4. doi: 10.1002/ajh.24174
- Ozgu Yurttas N, Eskazan AE. Dasatinib-induced pulmonary arterial hypertension. *Br J Clin Pharmacol*. (2018) 84:835–45. doi: 10.1111/bcp.13508
- Weatherald J, Chaumais MC, Savale L, Jais X, Seferian A, Canuet M, et al. Long-term outcomes of dasatinib-induced pulmonary arterial hypertension: a population-based study. *Eur Respir J*. (2017) 50:1700217. doi: 10.1183/13993003.00217-2017
- Daccord C, Letovanec I, Yerly P, Bloch J, Ognia A, Nicod LP, et al. First histopathological evidence of irreversible pulmonary vascular disease in dasatinib-induced pulmonary arterial hypertension. *Eur Respir J*. (2018) 51:1701694. doi: 10.1183/13993003.01694-2017
- Weatherald J, Chaumais MC, Montani D. Pulmonary arterial hypertension induced by tyrosine kinase inhibitors. *Curr Opin Pulm Med*. (2017) 23:392–7. doi: 10.1097/MCP.0000000000000412
- Simonneau G, Montani D, Celermajer DS, Denton CP, Gatzoulis MA, Krowka M, et al. Haemodynamic definitions and updated clinical classification of pulmonary hypertension. *Eur Respir J*. (2019) 53:1801913. doi: 10.1183/13993003.01913-2018
- Guignabert C, Phan C, Seferian A, Huertas A, Tu L, Thuillet R, et al. Dasatinib induces lung vascular toxicity and predisposes to pulmonary hypertension. *J Clin Invest*. (2016) 126:3207–18. doi: 10.1172/JCI86249
- Veith C, Schermuly RT, Brandes RP, Weissmann N. Molecular mechanisms of hypoxia-inducible factor-induced pulmonary arterial smooth muscle cell alterations in pulmonary hypertension. *J Physiol*. (2016) 594:1167–77. doi: 10.1113/JP270689
- Yu AY, Shimoda LA, Iyer NV, Huso DL, Sun X, McWilliams R, et al. Impaired physiological responses to chronic hypoxia in mice partially deficient for hypoxia-inducible factor 1 α . *J Clin Invest*. (1999) 103:691–6. doi: 10.1172/JCI5912
- Ball MK, Waypa GB, Mungai PT, Nielsen JM, Czech L, Dudley VJ, et al. Regulation of hypoxia-induced pulmonary hypertension by vascular smooth muscle hypoxia-inducible factor-1 α . *Am J Respir Crit Care Med*. (2014) 189:314–24. doi: 10.1164/rccm.201302-0302OC

12. Groeneveldt JA, Gans SJ, Bogaard HJ, Vonk-Noordegraaf A. Dasatinib-induced pulmonary arterial hypertension unresponsive to PDE-5 inhibition. *Eur Respir J.* (2013) 42:869–70. doi: 10.1183/09031936.00035913
13. Pyne NJ, Pyne S. Sphingosine kinase 1: a potential therapeutic target in pulmonary arterial hypertension? *Trends Mol Med.* (2017) 23:786–98. doi: 10.1016/j.molmed.2017.07.001
14. Wong CM, Bansal G, Pavlickova L, Marcocci L, Suzuki YJ. Reactive oxygen species and antioxidants in pulmonary hypertension. *Antioxid Redox Signal.* (2013) 18:1789–96. doi: 10.1089/ars.2012.4568
15. Farias JG, Herrera EA, Carrasco-Pozo C, Sotomayor-Zarate R, Cruz G, Morales P, et al. Pharmacological models and approaches for pathophysiological conditions associated with hypoxia and oxidative stress. *Pharmacol Ther.* (2016) 158:1–23. doi: 10.1016/j.pharmthera.2015.11.006
16. Astorga CR, Gonzalez-Candia A, Candia AA, Figueroa EG, Canas D, Ebensperger G, et al. Melatonin decreases pulmonary vascular remodeling and oxygen sensitivity in pulmonary hypertensive Newborn lambs. *Front Physiol.* (2018) 9:185. doi: 10.3389/fphys.2018.00185
17. Smukowska-Gorynia A, Rzymiski P, Marcinkowska J, Poniedzialek B, Komosa A, Cieslewicz A, et al. Prognostic value of oxidative stress markers in patients with pulmonary arterial or chronic thromboembolic pulmonary hypertension. *Oxid Med Cell Longev.* (2019) 2019:3795320. doi: 10.1155/2019/3795320
18. Jin H, Wang Y, Zhou L, Liu L, Zhang P, Deng W, et al. Melatonin attenuates hypoxic pulmonary hypertension by inhibiting the inflammation and the proliferation of pulmonary arterial smooth muscle cells. *J Pineal Res.* (2014) 57:442–50. doi: 10.1111/jpi.12184
19. Cardinali DP, Golombek DA, Rosenstein RE, Brusco LI, Vigo DE. Assessing the efficacy of melatonin to curtail benzodiazepine/Z drug abuse. *Pharmacol Res.* (2016) 109:12–23. doi: 10.1016/j.phrs.2015.08.016
20. Sanchez-Hidalgo M, Lee M, de la Lastra CA, Guerrero JM, Packham G. Melatonin inhibits cell proliferation and induces caspase activation and apoptosis in human malignant lymphoid cell lines. *J Pineal Res.* (2012) 53:366–73. doi: 10.1111/j.1600-079X.2012.01006.x
21. Farhood B, Goradel NH, Mortezaee K, Khanlarkhani N, Najafi M, Sahebkar A. Melatonin and cancer: from the promotion of genomic stability to use in cancer treatment. *J Cell Physiol.* (2019) 234:5613–27. doi: 10.1002/jcp.27391
22. Krestinina O, Fadeev R, Lomovsky A, Baburina Y, Kobayakova M, Akatov V. Melatonin can strengthen the effect of retinoic acid in HL-60 cells. *Int J Mol Sci.* (2018) 19:2873. doi: 10.3390/ijms19102873
23. Zhang X, Xia Q, Wei R, Song H, Mi J, Lin Z, et al. Melatonin protects spermatogonia from the stress of chemotherapy and oxidation via eliminating reactive oxidative species. *Free Radic Biol Med.* (2019) 137:74–86. doi: 10.1016/j.freeradbiomed.2019.04.009
24. Tengattini S, Reiter RJ, Tan DX, Terron MP, Rodella LF, Rezzani R. Cardiovascular diseases: protective effects of melatonin. *J Pineal Res.* (2008) 44:16–25. doi: 10.1111/j.1600-079X.2007.00518.x
25. Cipolla-Neto J, Amaral FGD. Melatonin as a hormone: new physiological and clinical insights. *Endocr Rev.* (2018) 39:990–1028. doi: 10.1210/er.2018-00084
26. Gomes Domingos AL, Hermsdorff HHM, Bressan J. Melatonin intake and potential chronobiological effects on human health. *Crit Rev Food Sci Nutr.* (2019) 59:133–40. doi: 10.1080/10408398.2017.1360837
27. Zhang J, Lu X, Liu M, Fan H, Zheng H, Zhang S, et al. Melatonin inhibits inflammasome-associated activation of endothelium and macrophages attenuating pulmonary arterial hypertension. *Cardiovasc Res.* (2020) 116:2156–69. doi: 10.1093/cvr/cvz312
28. Chen F, Li X, Aquadro E, Haigh S, Zhou J, Stepp DW, et al. Inhibition of histone deacetylase reduces transcription of NADPH oxidases and ROS production and ameliorates pulmonary arterial hypertension. *Free Radic Biol Med.* (2016) 99:167–78. doi: 10.1016/j.freeradbiomed.2016.08.003
29. Jin H, Liu M, Zhang X, Pan J, Han J, Wang Y, et al. Grape seed procyanidin extract attenuates hypoxic pulmonary hypertension by inhibiting oxidative stress and pulmonary arterial smooth muscle cells proliferation. *J Nutr Biochem.* (2016) 36:81–8. doi: 10.1016/j.jnutbio.2016.07.006
30. Liu M, Liu Q, Pei Y, Gong M, Cui X, Pan J, et al. Aqp-1 gene knockout attenuates hypoxic pulmonary hypertension of mice. *Arterioscler Thromb Vasc Biol.* (2019) 39:48–62. doi: 10.1161/ATVBAHA.118.311714
31. Adesina SE, Kang BY, Bijli KM, Ma J, Cheng J, Murphy TC, et al. Targeting mitochondrial reactive oxygen species to modulate hypoxia-induced pulmonary hypertension. *Free Radic Biol Med.* (2015) 87:36–47. doi: 10.1016/j.freeradbiomed.2015.05.042
32. Chen PI, Cao A, Miyagawa K, Tojais NF, Hennigs JK, Li CG, et al. Amphetamines promote mitochondrial dysfunction and DNA damage in pulmonary hypertension. *JCI Insight.* (2017) 2:e90427. doi: 10.1172/jci.insight.90427
33. Bhansali S, Sohi K, Dhawan V. Hypoxia-induced mitochondrial reactive oxygen species (mtROS) differentially regulates smooth muscle cell (SMC) proliferation of pulmonary and systemic vasculature. *Mitochondrion.* (2020) 57:97–107. doi: 10.1016/j.mito.2020.11.012
34. Liu, J., Wang, W., Wang, L., Chen, S., Tian, B., Huang, K., et al. (2018). IL-33 initiates vascular remodeling in hypoxic pulmonary hypertension by up-regulating HIF-1 α and VEGF expression in vascular endothelial cells. *EBioMedicine* 33, 196–210. doi: 10.1016/j.ebiom.2018.06.003
35. Pullamsetti SS, Mamazhakypov A, Weissmann N, Seeger W, Savai R. Hypoxia-inducible factor signaling in pulmonary hypertension. *J Clin Invest.* (2020) 130:5638–51. doi: 10.1172/JCI137558
36. Joppa P, Petrasova D, Stancak B, Dorkova Z, Tkacova R. Oxidative stress in patients with COPD and pulmonary hypertension. *Wien Klin Wochenschr.* (2007) 119:428–34. doi: 10.1007/s00508-007-0819-y
37. Turck P, Fraga S, Salvador I, Campos-Carraro C, Lacerda D, Bahr A, et al. Blueberry extract decreases oxidative stress and improves functional parameters in lungs from rats with pulmonary arterial hypertension. *Nutrition.* (2020) 70:110579. doi: 10.1016/j.nut.2019.110579
38. Reiter RJ, Tan DX, Galano A. Melatonin: exceeding expectations. *Physiology (Bethesda).* (2014) 29:325–33. doi: 10.1152/physiol.00011.2014
39. Bowers R, Cool C, Murphy RC, Tudor RM, Hopken MW, Flores SC, et al. Oxidative stress in severe pulmonary hypertension. *Am J Respir Crit Care Med.* (2004) 169:764–9. doi: 10.1164/rccm.200301-147OC
40. Archer SL, Marsboom G, Kim GH, Zhang HJ, Toth PT, Svensson EC, et al. Epigenetic attenuation of mitochondrial superoxide dismutase 2 in pulmonary arterial hypertension: a basis for excessive cell proliferation and a new therapeutic target. *Circulation.* (2010) 121:2661–71. doi: 10.1161/CIRCULATIONAHA.109.916098
41. Gonzalez-Candia A, Veliz M, Carrasco-Pozo C, Castillo RL, Cardenas JC, Ebensperger G, et al. Antenatal melatonin modulates an enhanced antioxidant/pro-oxidant ratio in pulmonary hypertensive newborn sheep. *Redox Biol.* (2019) 22:101128. doi: 10.1016/j.redox.2019.101128
42. Reis GS, Augusto VS, Silveira AP, Jordao AA Jr, Baddini-Martinez J, Poli Neto O, et al. Oxidative-stress biomarkers in patients with pulmonary hypertension. *Pulm Circ.* (2013) 3:856–61. doi: 10.1086/674764
43. Zhang S, Yang T, Xu X, Wang M, Zhong L, Yang Y, et al. Oxidative stress and nitric oxide signaling related biomarkers in patients with pulmonary hypertension: a case control study. *BMC Pulm Med.* (2015) 15:50. doi: 10.1186/s12890-015-0045-8
44. Green DE, Murphy TC, Kang BY, Kleinhenz JM, Szyndralewicz C, Page P, et al. The Nox4 inhibitor GKT137831 attenuates hypoxia-induced pulmonary vascular cell proliferation. *Am J Respir Cell Mol Biol.* (2012) 47:718–26. doi: 10.1165/rcmb.2011-0418OC
45. Semenza GL. Oxygen sensing, hypoxia-inducible factors, and disease pathophysiology. *Annu Rev Pathol.* (2014) 9:47–71. doi: 10.1146/annurev-pathol-012513-104720
46. Guo X, Fan Y, Cui J, Hao B, Zhu L, Sun X, et al. NOX4 expression and distal arteriolar remodeling correlate with pulmonary hypertension in COPD. *BMC Pulm Med.* (2018) 18:111. doi: 10.1186/s12890-018-0680-y
47. Kracun D, Klop M, Knirsch A, Petry A, Kanchev I, Chalupsky K, et al. NADPH oxidases and HIF1 promote cardiac dysfunction and pulmonary hypertension in response to glucocorticoid excess. *Redox Biol.* (2020) 34:101536. doi: 10.1016/j.redox.2020.101536
48. Fazakas C, Nagaraj C, Zabini D, Vegh AG, Marsh LM, Wilhelm I, et al. Rho-kinase inhibition ameliorates dasatinib-induced endothelial dysfunction and pulmonary hypertension. *Front Physiol.* (2018) 9:537. doi: 10.3389/fphys.2018.00537
49. Kurakula K, Smolders V, Tura-Ceide O, Jukema JW, Quax PHA, Goumans MJ. Endothelial dysfunction in pulmonary hypertension: cause or consequence? *Biomedicines.* (2021) 9:57. doi: 10.3390/biomedicines9010057
50. Bourgeois A, Omura J, Habbout K, Bonnet S, Boucherat O. Pulmonary arterial hypertension: new pathophysiological insights and emerging therapeutic

- targets. *Int J Biochem Cell Biol.* (2018) 104:9–13. doi: 10.1016/j.biocel.2018.08.015
51. Thompson AAR, Lawrie A. Targeting vascular remodeling to treat pulmonary arterial hypertension. *Trends Mol Med.* (2017) 23:31–45. doi: 10.1016/j.molmed.2016.11.005
 52. Dai Z, Zhu MM, Peng Y, Jin H, Machireddy N, Qian Z, et al. Endothelial and smooth muscle cell interaction via FoxM1 signaling mediates vascular remodeling and pulmonary hypertension. *Am J Respir Crit Care Med.* (2018) 198:788–802. doi: 10.1164/rccm.201709-1835OC
 53. Humbert M, Guignabert C, Bonnet S, Dorfmüller P, Klinger JR, Nicolls MR, et al. Pathology and pathobiology of pulmonary hypertension: state of the art and research perspectives. *Eur Respir J.* (2019) 53:1801887. doi: 10.1183/13993003.01887-2018
 54. Mandras SA, Mehta HS, Vaidya A. Pulmonary hypertension: a brief guide for clinicians. *Mayo Clin Proc.* (2020) 95:1978–88. doi: 10.1016/j.mayocp.2020.04.039
 55. Zeng DX, Liu XS, Xu YJ, Wang R, Xiang M, Xiong WN, et al. Plasmid-based short hairpin RNA against cyclin D1 attenuated pulmonary vascular remodeling in smoking rats. *Microvasc Res.* (2010) 80:116–22. doi: 10.1016/j.mvr.2010.03.002
 56. Mei L, Zheng YM, Song T, Yadav VR, Joseph LC, Truong L, et al. Rieske iron-sulfur protein induces FKBP12.6/RyR2 complex remodeling and subsequent pulmonary hypertension through NF- κ B/cyclin D1 pathway. *Nat Commun.* (2020) 11:3527. doi: 10.1038/s41467-020-17314-1
 57. Satoh K, Nigro P, Berk BC. Oxidative stress and vascular smooth muscle cell growth: a mechanistic linkage by cyclophilin A. *Antioxid Redox Signal.* (2010) 12:675–82. doi: 10.1089/ars.2009.2875
 58. Durgin BG, Straub AC. Redox control of vascular smooth muscle cell function and plasticity. *Lab Invest.* (2018) 98:1254–62. doi: 10.1038/s41374-018-0032-9
 59. Semenza GL. Hypoxia-inducible factors in physiology and medicine. *Cell.* (2012) 148:399–408. doi: 10.1016/j.cell.2012.01.021
 60. Blum JI, Bijli KM, Murphy TC, Kleinhenz JM, Hart CM. Time-dependent PPAR γ modulation of HIF-1 α signaling in hypoxic pulmonary artery smooth muscle cells. *Am J Med Sci.* (2016) 352:71–9. doi: 10.1016/j.amjms.2016.03.019
 61. Naji L, Carrillo-Vico A, Guerrero JM, Calvo JR. Expression of membrane and nuclear melatonin receptors in mouse peripheral organs. *Life Sci.* (2004) 74:2227–36. doi: 10.1016/j.lfs.2003.08.046
 62. Torres F, Gonzalez-Candia A, Montt C, Ebensperger G, Chubretovic M, Seron-Ferre M, et al. Melatonin reduces oxidative stress and improves vascular function in pulmonary hypertensive newborn sheep. *J Pineal Res.* (2015) 58:362–73. doi: 10.1111/jpi.12222
 63. Masana MI, Doolen S, Ersahin C, Al-Ghoul WM, Duckles SP, Dubocovich ML, et al. MT(2) melatonin receptors are present and functional in rat caudal artery. *J Pharmacol Exp Ther.* (2002) 302:1295–302. doi: 10.1124/jpet.302.3.1295
- Conflict of Interest:** The authors declare that the research was conducted in the absence of any commercial or financial relationships that could be construed as a potential conflict of interest.
- Publisher's Note:** All claims expressed in this article are solely those of the authors and do not necessarily represent those of their affiliated organizations, or those of the publisher, the editors and the reviewers. Any product that may be evaluated in this article, or claim that may be made by its manufacturer, is not guaranteed or endorsed by the publisher.
- Copyright © 2022 Wang, Pan, Han, Gong, Liu, Zhang, Liu, Wang, Tang, Wu, Wang, Yan, Li and Yuan. This is an open-access article distributed under the terms of the Creative Commons Attribution License (CC BY). The use, distribution or reproduction in other forums is permitted, provided the original author(s) and the copyright owner(s) are credited and that the original publication in this journal is cited, in accordance with accepted academic practice. No use, distribution or reproduction is permitted which does not comply with these terms.